

Introduction

In these last years, many aspects about FWI have been studied concerning the formulation of efficient modelling algorithms and inversion procedures (Virieux et al. 2009) (Fichtner 2010) (Warner and Guasch 2016) just to cite some works. However, its application to real data requires applying specific operations on the seismograms to obtain observed data that can be reproduced by the modelling algorithm in a reliable and consistent way. These processing steps are needed in the different phases of the inversion: at the beginning to estimate a starting model as close as possible to the valley of the global minimum of the misfit function, and successively during the local FWI procedure, to enhance the resolution of the previously estimated velocity field. Different methodologies have been developed to estimate an accurate velocity field to start the FWI, for example, travel-time tomography and migration velocity analysis. Unfortunately, they require a considerable manpower effort.

In this work, we perform a complete procedure of acoustic FWI inversion starting from a 1D velocity model and applying a global optimization procedure on a coarse inversion grid (Sajeva et al. 2016) followed by a local gradient-based FWI to improve the resolution of the velocity field. To increase the robustness of the inversion, we consider a data misfit based on the L^1 -norm difference between the predicted and the observed envelope seismogram, relaxing the need of accurate knowledge of the source wavelet and reducing possible cycle-skipping effects. To validate the final model, we pre-stack depth migrate the data using the final estimated velocity field, and we check the improvements on the flattening of the events in the common-image-gathers (CIGs).

The seismic data for the inversion procedure

The seismic data pertains to an inline extracted from a 3D marine volume, acquired by ENI. The entire profile consists of 765 shots spaced 12.5 m with 159 channels each, employing an air-gun source. The group interval is 25 m, and the resulting offset for the shots ranges between 150 m and 4.1 km approximately. The total length of the line is about 11.2 km. The time sampling is 4 ms, and the time length is 2.6 s. The seabed is considered flat with a depth of approximately 300m.

To reduce the computational cost of the FWI, we consider the data between the CDP 161 and 737, for a total length of about 7.2km. In this region, we select only 56 shot gathers, obtained by a mean of 5 adjacent shot gathers, distributed with a uniform distance of 125m. Figure 1a shows a sketch of the geometry acquisition: the red arrow represents the part of the profile used for the inversion, whereas the black and red points represent the position of the sources considered. In this way, the number of traces for shot gather changes from a minimum of 7 traces for the first shot to a maximum of 159 for the shots between the 16th and 56th, for a total number of 6517 traces. Figure 1b shows three shot gathers located at the begin, in the middle and at the end of the segment, respectively. The red lines in Figure 1b enclose a specific time window, which varies from a minimum of 0.1 s to a maximum of 0.5 s, designed to focus the inversion on the diving waves and the shallow reflections. Finally, the input data is band-filtered in the range 0-10 Hz and a trace-by-trace normalization is applied to enforce the information at long offset. The misfit function we consider is the L^1 -norm difference between the predicted and the observed envelopes of the seismograms.

Modelling

The synthetic data are computed using an explicit finite difference algorithm used to solve the 2D acoustic wave equation (Galuzzi et al. 2017) where the order of approximation of the spatial derivatives is optimized to reduce the numerical dispersion. The model dimensions are approximately 7 km in length, and 2.4 km in depth and the modelling grid is made by 242x80 nodes, with a uniform grid size of $dx=30m$. The seabed is therefore located between the 10th and the 11th row of the grid. The source wavelet is estimated from the sea-bed reflection.

Estimation of an initial model by means of Genetic Algorithms

The initial model used in this work is obtained by a global optimization procedure that uses the genetic algorithms on a coarse inversion grid (Tognarelli et al. 2015) (Mazzotti et al. 2017). The coarse grid

consists of 4840 nodes, organized in 40 rows. The first row of the inversion grid is located at the sea-surface, and the first five rows represent the sea layer characterized by a constant velocity of 1480 m/s. The total number of unknowns is therefore 3880. To tackle this inversion problem, the genetic algorithms are applied in a layer stripping procedure focusing at the beginning on the upper part (down to a depth of 1.5 km), then on the lower part (down to 2.4 km) and finally on the whole model for a refinement. The use of a coarse grid reduces the number of unknowns of the global optimization (that otherwise would be 16940) and helps the misfit function to be more sensitive to the model variations. The GA parameters are set as follow: 4800 individuals, a selection rate of 0.42 (to limit the computational time for each generation) and a mutation rate of 0.1%. The search range for GA is 800 m/s centred on the 1D velocity model obtained as a horizontal mean of the model computed in Mazzotti et al. 2017. Figure 2a shows the best GA model after approximately 600 generations.

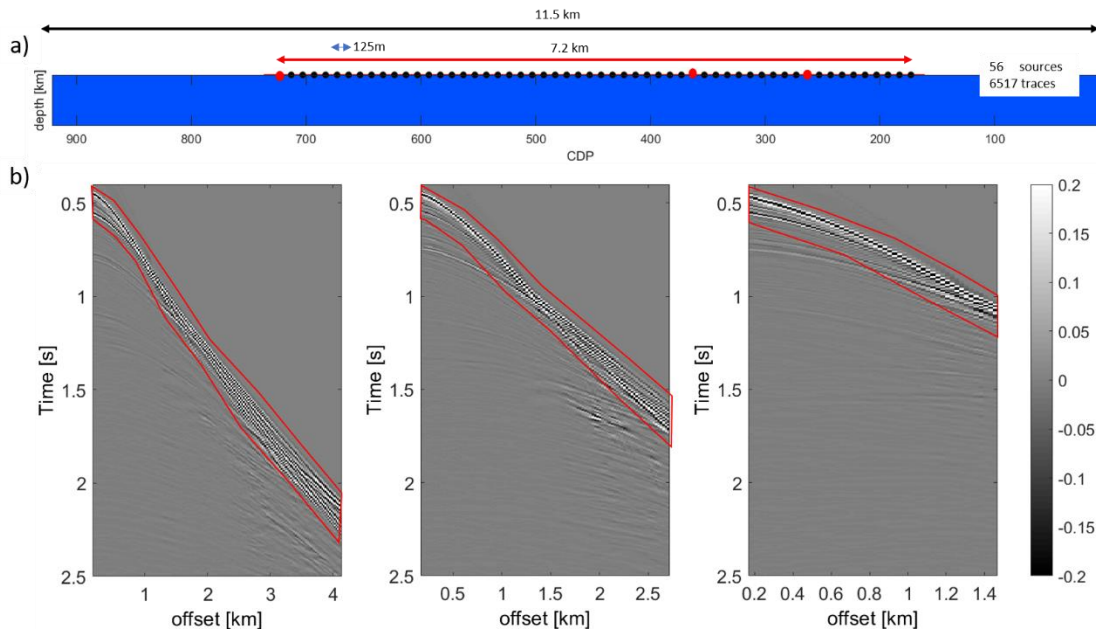


Figure 1: a) Sketch of the seismic acquisition: the points represent the 56 sources considered for the inversion; b) three shot gathers used for the inversion at the begin, middle and end of the studied profile (red dots in Fig. 1a). The red windows delineate the data used in the inversion.

Inversion procedure and results

As a local optimization method, we use the steepest descend algorithm, starting from the best GA model showed in Figure 2a. The gradient of the misfit function is computed using the adjoint method (Plessix, 2006, Fichtner 2010). The unknowns are the velocity values at the modelling grid nodes situated below the sea layer, for a total of 242×70 unknowns. The velocities range between 1300 m/s and 3750 m/s. We perform 50 iterations of the minimization procedure.

Figure 2b shows the final model obtained at the end of the local inversion process. The main characteristics of the GA velocity model are preserved; however, a higher resolution is achieved that highlights a velocity inversion around a depth of 1.2 km in the centre of the model. Figure 3 shows two shot gathers (left frames) and the difference between the observed and predicted data before (central frames) and after (right frames) the local optimization procedure. A decrease of the misfit is clear in both gathers, in particular at far offset.

Finally, Figure 4 shows the CIGs obtained by pre-stack depth migrating the data, using the final velocity model. A good horizontal alignment of the events can be noted, especially for the events just below the seabed reflection and located in the central part of the model.

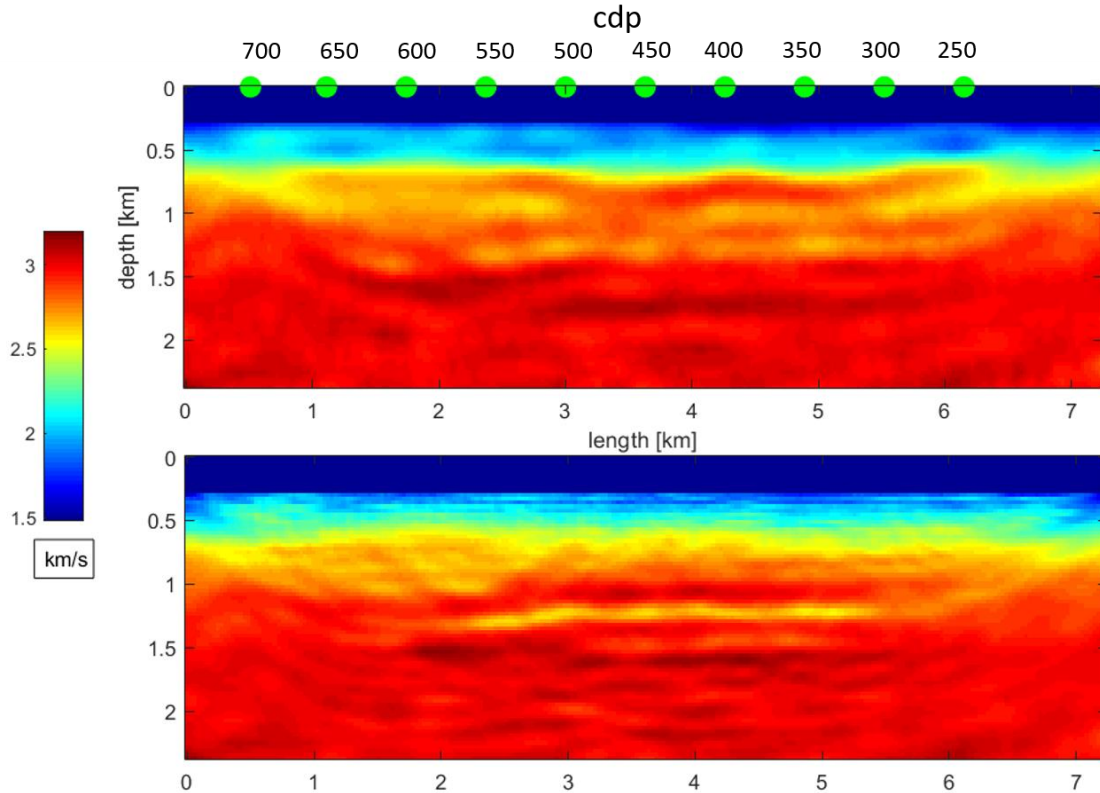


Figure 2: a) Best GA model obtained at the end of the global optimization procedure on the coarse grid; b) Final model obtained at the end of the local optimization procedure.

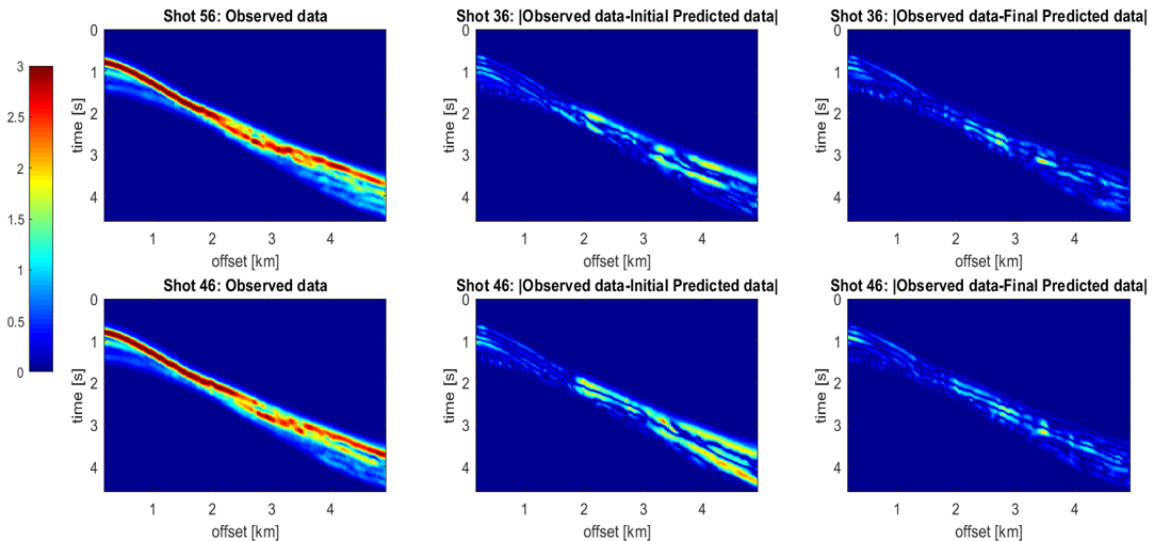


Figure 3: Observed data for two shot gathers (left) and the difference between the predicted and the observed data before (center) and after (right) the local inversion.

Conclusions

In this work, we make an exercise of acoustic FWI application on a 2D real dataset extracted from a 3D volume using the envelope of the diving waves to increase the robustness of the inversion. The whole procedure is divided into a global and a local optimization step, aimed at estimating an initial velocity model and at increasing its resolution. The high number of unknowns in the GA global optimization allows to evidence lateral and vertical velocity variations in the estimated model, which are successively refined by the local optimization. In this test no other a priori information is available, so the reliability

of the inversion is based only on the horizontal alignment of the reflections observed in CIG. The outcomes show that, at least to a depth of 1.5 km, the horizontal alignment can be judged satisfactory, considering that the manpower effort has been limited to just some pre-processing steps (filtering, muting, envelope computation) and the setting up of the inversion parameters for GA and local inversion.

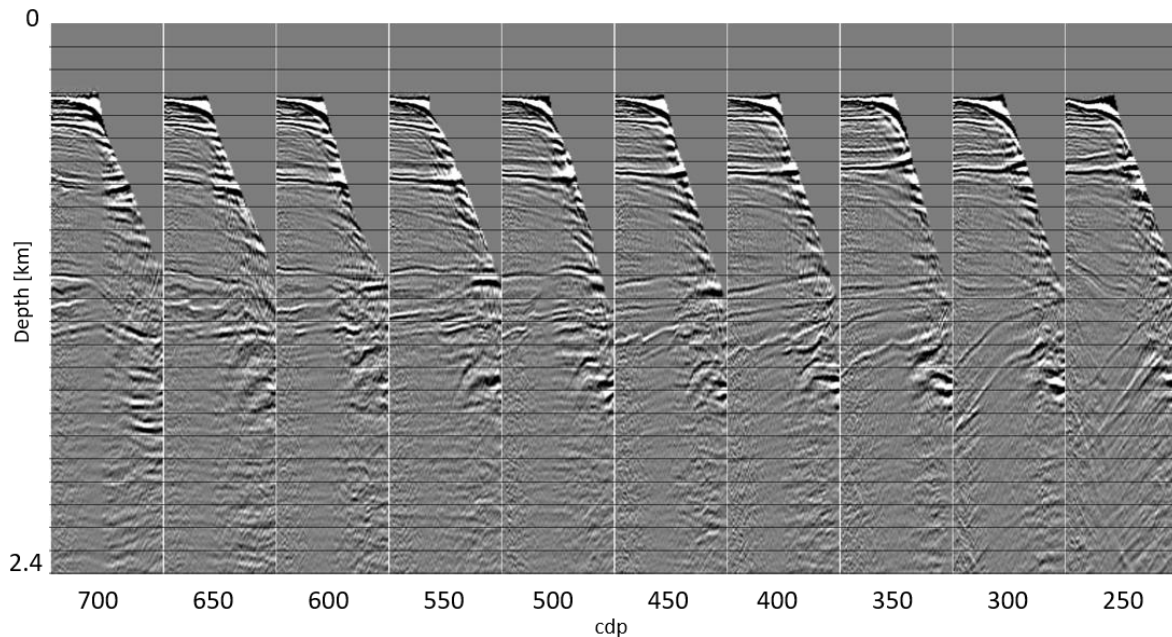


Figure 4: CIGs derived from PSDM (Kirchhoff) using the final velocity model obtained at the end of the local optimization procedure. CIG maximum offset is 2 km.

Acknowledgements

The authors wish to thank Eni for its continued support in the research. The seismic data processing and the CIGs computation were carried out using the Promax software of Landmark Graphics Corporation that is gratefully acknowledged.

References

- Fichtner, A. [2011] Full Seismic Waveform Modelling and Inversion. *Springer Science & Business Media*.
- Galuzzi B., Zampieri E., Stucchi E. [2017] A local adaptive method for the numerical approximation in seismic wave modelling. *Communications in Applied and Industrial Mathematics*, **8**, no. 1, pp. 265-281.
- Mazzotti A., Bienati N., Stucchi E., Tognarelli A., Aleardi M. and Sajeve A. [2017] Two-grid genetic algorithm full-waveform inversion. *The Leading Edge*, **35**, pp. 1068-1075.
- Plessix R. [2006] A review of the adjoint-state method for computing the gradient of a functional with geophysical applications. *Geophysical Journal International*, **167**, no. 2, pp. 495-503.
- Sajeve, A., Bienati, N., Aleardi, M., Stucchi, E., Bienati, N. and Mazzotti, A. [2016] Estimation of acoustic macro-models using a genetic full-waveform inversion: applications to the Marmousi model. *Geophysics*, **81**, no. 4, pp. R173-R184.
- Tognarelli, A., Stucchi, E., Bienati, N., Sajeve, A., Aleardi, M. and Mazzotti, A. [2015] Two-grid stochastic full waveform inversion of 2D marine seismic data. 77th Conference & Exhibition, EAGE, Expanded Abstract.
- Virieux, J. and Operto, S. [2009] An overview of full waveform inversion in exploration geophysics. *Geophysics*, **74**, no. 6, pp. 27-152.
- Warner, M., Guasch L. [2016] Adaptive waveform inversion: Theory. *Geophysics*, **81**, no. 6, R429-R445.